Detecting dimensional crossover and finite Hilbert space through entanglement entropies

Mariano Garagiola,[*] Eloisa Cuestas,[†] Federico M. Pont,[‡] Pablo Serra,[§] and Omar Osenda[‖]
Facultad de Matemática, Astronomía y Física, Universidad Nacional de Córdoba and IFEG-CONICET, Ciudad Universitaria, X5000HUA Córdoba, Argentina
(Received 11 February 2016; published 19 October 2016)

The information content of the two-particle one- and two-dimensional Calogero model is studied by using the von Neumann and Rényi entropies. The one-dimensional model is shown to have nonmonotonic entropies with finite values in the large-interaction-strength limit. On the other hand, the von Neumann entropy of the two-dimensional model with isotropic confinement is a monotone increasing function of the interaction strength which diverges logarithmically. By considering an anisotropic confinement in the two-dimensional case we show that the one-dimensional behavior is eventually reached when the anisotropy increases. The crossover from two to one dimensions is demonstrated by using the harmonic approximation and it is shown that the von Neumann divergence only occurs in the isotropic case. The Rényi entropies are used to highlight the structure of the model spectrum. In particular, it is shown that these entropies have a nonmonotonic and nonanalytical behavior in the neighborhood of the interaction strength parameter values where the Hilbert space and, consequently, the spectrum of the reduced density matrix are both finite.

DOI: 10.1103/PhysRevA.94.042115

I. INTRODUCTION

In the last few years there has been a growing interest in models of many interacting particles with continuous variables [1,2]. This interest is fueled by, on one hand, some unexpected physical traits shown by the models and, on the other hand, that they can be analytically treated to a great extent providing exact solutions based on which one can assess approximate ones [3].

Among the unexpected physical traits can be mentioned the closeness between the occupation numbers of systems formed by bosons or fermions in the appropriate regime [4]. In this context, the occupation number of a natural orbital refers to the eigenvalue and corresponding eigenvector of a given reduced density matrix associated with the quantum state of the system. We identify natural occupation numbers with the eigenvalues of a reduced density matrix since they only differ in a constant multiplicative factor: the number of particles that constitute the system.

Even for those models with continuous variables where the spectrum, the ground state and, in some cases, the excited states of an N-particle system are exactly known, the reduced density matrices that describe the quantum state of a subset of p particles are rather difficult to calculate.

If $N - p$ particles are traced out from the density matrix associated with a quantum system with N particles, the matrix obtained is usually called a p-reduced density matrix, or p-RDM. The p-RDM allows us to study a number of physical quantities as the natural orbital with its occupation numbers as well as different kinds of quantum entropies. Unfortunately, situations where exact p-RDM can be obtained [4–8] are even more scarce than those where exact spectrum or eigenstates are available. The cases where a p-RDM can be obtained exactly, like the Moshinsky [9], Calogero [10], and Calogero–Sutherland [11] models, show clearly the difficulties involved.

The Calogero model, its eigenstates and spectrum, were known to be related to many other problems in physics, a trademark recognized from the very beginning of the subject. In this respect, the pioneering work of Sutherland pointed out that the probability distribution of the ground-state function for the N-particle model was identical to the joint probability density function for the eigenvalues of random ensembles. In particular, by changing the interaction parameter it was possible to recover the orthogonal, unitary, and symplectic ensemble density functions [11]. This result was first explained as merely arising from the Jastrow factor present in the ground-state function, but the relationship was demonstrated to be deeper than what was originally thought—see Ref. [12] where it is shown that the correspondence can be extended to response functions or correlations of the density of states of a quantum chaotic system [13].

At the same time, the relationship of the Calogero model with the fractionary quantum Hall effect was well established—see, for instance, the work by Azuma and Iso [14]. It was also understood that the Calogero particles are basically free but obey generalized fractional exclusion statistics [15]. So, when referring to bosons or fermions in the one- or two-dimensional Calogero model, it is the symmetry of the eigenfunctions that dictates the terminology since the permutation group in two dimensions allows more possibilities to the particles. This argument explains why the interaction-strength parameter is sometimes termed the "statistics parameter."

Following the terminology used by Polychronakos [16], the freezing trick is the bridge between the Calogero model and lattice integrable systems of the Haldane–Shastry type [17]. It is worth mentioning that the trick, which is essentially a large interaction-strength limit, works well when the particles have well-defined isolated classical equilibrium positions, as is the case of the one-dimensional Calogero model with or without periodic boundary conditions.

[*]mgaragiola@famaf.unc.edu.ar
[†]mecuestas@famaf.unc.edu.ar
[‡]pont@famaf.unc.edu.ar
[§]serra@famaf.unc.edu.ar
[‖]osenda@famaf.unc.edu.ar

Summarizing, the Calogero model has been widely studied from condensed-matter physics through group theory and has experienced several revivals, which is why looking for new physics in it seems always tempting and is rewarding, as we will see.

More recently, the availability of exact p-RDM [4] or very good checkable approximations to it [7,18] has constituted a significant tool to shed some light over the behavior of natural occupation numbers in fermion systems and their relationship with some generalizations of the exclusion principle [19,20].

The number of nonzero occupation numbers and how fast they become negligible are excellent quantifiers to evaluate if an approximate method which involves an expansion over a finite functional basis has a good chance to succeed. Of course, it is in general impossible to know *a priori* how many (if any) natural occupation numbers (NONs) become zero for a given multipartite Hamiltonian. Moreover, it is widely accepted that the presence of Coulomb "cusps" leads, inevitably, to an infinite set of nonzero NONs [21].

Furthermore, the same availability of exact p-RDMs develops some unexpected features. As has been said above, fermion systems usually have an infinite number of nontrivial NONs. But, as some of us found quite recently, the Calogero model in one dimension has a finite number of nonzero NONs for a discrete set of values of the interaction parameter [4]. To obtain this result it is crucial to realize that the p-RDM of a system of N particles described by the Calogero model can be written exactly as a finite matrix whose entries can be obtained analytically. The dimension of the matrix depends on p, N, the interaction parameter, and if the particles are fermions or bosons.

Another feature found in Ref. [4] is related to the behavior of the von Neumann entropy (vNE) obtained from the NONs of one-dimensional systems with different numbers of particles. In all cases, the vNE was found to be a nonmonotonic function of the interaction strength, showing a maximum for some finite value of the interaction strength.

There are numerous examples which show that different entanglement entropies associated with p-RDM obtained from ground-state wave functions of two- and three-dimensional problems are monotonic functions of the interaction strength between the particles [22,23]. Moreover, the closely related entanglement properties of fractional quantum Hall liquids obtained from the Laughlin wave function also support the monotonic behavior. This has been studied in the works by Zeng *et al.* [24], Iblisdir *et al.* [25], and Haque *et al.* [26]. Let us remember that the Laughlin wave function for n particles and $1/m$ filling factor has exactly the same form as the ground-state function of the one-dimensional Calogero model for n particles in one dimension with interaction strength $m(m-1)$. Anyway, it is prudent not get carried away by the similarities, since the partition made to obtain the p-RDM will determine between which subsystems the entanglement is calculated and a partition between Calogero particles in one or two dimensions is not equivalent to a partition between particles described by the Laughlin wave function.

The aim of the present work is to study a few entanglement entropies as functions of interaction strength for the one- and two-dimensional two-particle Calogero model. We consider a continuous interaction-strength parameter, in this way the ground-state wave function is exact but the one-particle reduced density matrix (1-RDM) and its spectrum are not necessarily so. The large interaction limit will allow us to show that the one-dimensional model has always a finite entanglement entropy in contradistinction to the divergent behavior observed in two or larger dimensions. In particular, we show that the change from one- to two-dimensional behavior can be characterized as a crossover or, more precisely, the entanglement entropy of anisotropic Calogero systems in two dimensions behaves as one-dimensional or two-dimensional according to the amount of anisotropy and the interaction strength. It is also shown that the Rényi entanglement entropies are able to detect that the system has finite and exact solutions for some particular values of the interaction-strength parameter where the effective Hilbert space of the systems is also finite, a fact that is completely overlooked by the von Neumann entropy. We also discuss some inadequacy of the so-called linear entropy to study continuous variable systems in one or two dimensions.

The paper is organized as follows: In Sec. II we give some definitions and basic results for the Calogero model and entanglement entropies. In Sec. III, we calculate the spectrum and von Neumann entropy of the one-dimensional 1-RDM. Section IV is devoted to the Rényi entropies. The two-dimensional isotropic case is studied in Sec. V, while in Sec. VI the anisotropic case is treated in the large-interaction limit. We discuss the one- to two-dimensional crossover in Sec. VII. Finally, we discuss our findings and conclude in Sec. VIII.

II. PRELIMINARIES

The information content of a given bipartite pure quantum state $|\psi_{AB}\rangle$ can be studied by using different entanglement entropies, which are obtained from the reduced density matrix $\rho_A = \mathrm{Tr}_B(|\psi_{AB}\rangle\langle\psi_{AB}|)$.

In the case of a two-particle wave function $\Psi(\vec{x}_1,\vec{x}_2)$, where $\vec{x}_1, \vec{x}_2$ are the position vectors of the particles, the 1-RDM can be constructed by tracing out one of the particles:

$$\rho(\vec{x};\vec{y}) = \int \Psi^{\star}(\vec{x},\vec{z})\Psi(\vec{y},\vec{z})d\vec{z}. \tag{1}$$

Its eigenvalues λ_k are given by the following integral equation:

$$\int \rho(\vec{x};\vec{y})\phi_k(\vec{y})d\vec{y} = \lambda_k\phi_k(\vec{x}), \quad k = 1,2,3,\ldots. \tag{2}$$

One of the possible entanglement measure is the von Neumann entropy S_{vN}, which is given by

$$S_{vN}(\rho) = -\mathrm{Tr}(\rho\log_2\rho) = -\sum_k \lambda_k \log_2\lambda_k. \tag{3}$$

It is important to emphasize that it is not the only entanglement measure at our disposal. Another possible tool widely used to study entanglement in many-body or extended systems is the Rényi entropy

$$S^{\alpha}(\rho) = \frac{1}{1-\alpha}\log_2 \mathrm{Tr}\rho^{\alpha} = \frac{1}{1-\alpha}\log_2\left(\sum_k \lambda_k^{\alpha}\right). \tag{4}$$

This entanglement measure finds its natural place in information theory as a generalization of several other entropies (Shannon's, collision, etc.) which can be recovered for particular values of the parameter α. It is worth mentioning that, for a given probability distribution, the Rényi entropies defined as in Eq. (4) constitute a monoparametric family of convex functions for different choices of the parameter α.

The study of Rényi entanglement entropies has resulted in a better understanding of the entanglement in one-dimensional gases and spin chains [27–29]. There are a number of reasons to use the quantum Rényi entropies; the main two are (a) the vNE can be obtained as a limiting case when the parameter $\alpha \to 1$, and (b) the calculation of the Rényi entropies for many different values of the parameter α provides a better understanding of the distribution of the entanglement spectrum of a system than that obtained by considering only the von Neumann entropy.

Many authors also use the so-called linear entropy (LE) S_{le},

$$S_{le} = 1 - \mathrm{Tr}\rho^2, \tag{5}$$

which is mainly motivated by its ease of computation: for continuous variable systems the calculation of $\mathrm{Tr}\rho^2$ is reduced to just an integral. However, there are some reasons to suspect the quality of information provided by the linear entropy. For instance, no matter how entangled or how many particles are considered, in the large-interaction limit the linear entropy of the Calogero model always converges to unity, as in the case of the Moshinsky model [8,22].

The Calogero model

The two-particle Calogero Hamiltonian in dimension D [10] can be written as

$$H = h(1) + h(2) + \nu(\nu-1)\frac{1}{r_{12}^2}, \tag{6}$$

where $\vec{r}_{12} = \vec{x}_1 - \vec{x}_2$ denotes the relative separation between the particles, $\vec{x}_1$ and $\vec{x}_2$ are the positions of the particles, and $\nu(\nu-1)$ denotes the interaction strength as introduced by Sutherland [11]. The one-particle harmonic Hamiltonians have the following form:

$$h(i) = -\tfrac{1}{2}\nabla_i^2 + \tfrac{1}{2}r_i^2, \quad i = 1,2, \tag{7}$$

where units defined by $\hbar = 1$, $m = 1$, and $\omega = 1$ are used through the present work.

1. One-dimensional case

For two bosons the totally symmetric ground-state wave function and energy are given by

$$E = (\nu+1), \quad \psi_0^b(x_1,x_2) = C_{1,\nu}^b \Delta_\nu e^{-\frac{1}{2}(x_1^2+x_2^2)}, \tag{8}$$

where Δ_ν is the Jastrow factor

$$\Delta_\nu = |x_1 - x_2|^\nu, \tag{9}$$

while for two spinless fermions we have an antisymmetrical wave function

$$\psi_0^f(x_1,x_2) = C_{1,\nu}^f \mathrm{sign}(x_1 - x_2)\Delta_\nu e^{-\frac{1}{2}(x_1^2+x_2^2)}, \tag{10}$$

where $C_{1,\nu}^b$ and $C_{1,\nu}^f$ are normalization constants [30].

It has recently been shown that, for the boson (fermion) wave function with $\nu = 2n$ ($\nu = 2n-1$), $n \in \mathbb{N}$, the absolute value in Eq. (9) [Eq. (10)] can be ignored and the only integrals needed to find 1-RDM are Gaussian integrals with even (odd) powers in the Jastrow factor. Moreover, the 1-RDM (1) is then a Gaussian function times a multinomial expression of (x,y). In those cases, the general expression for $\rho_N^{(p)}$, which is quite cumbersome to obtain, can be written as a finite sum of Hermite functions [4].

2. Two and higher dimensions

In dimensions higher than two the exact ground-state wave function of bosons

$$\Psi_0^b = C_{D,\nu}^b |\vec{x}_1 - \vec{x}_2|^{\mu_b} e^{-\frac{1}{2}(r_1^2+r_2^2)}, \tag{11}$$

and fermions

$$\Psi_0^f = C_{D,\nu}^f |\vec{x}_1 - \vec{x}_2|^{\mu_f} \psi_S e^{-\frac{1}{2}(r_1^2+r_2^2)}, \tag{12}$$

are quite similar to the one-dimensional ones [31]. In Eqs. (11) and (12), the exponents μ_b and μ_f are functions of the interaction strength and the dimension D, and ψ_S is one of the 2×2 Slater determinants which are the $N = 2$ noninteracting fermion ground-state wave functions [31].

As in the one-dimensional case, the exact ground-state wave function for bosons and fermions cannot be obtained for the same set of parameters since

$$\mu_b = \tfrac{1}{2}\left(\sqrt{(D-2)^2 + 4\nu(\nu-1)} - (D-2)\right), \tag{13}$$

and

$$\mu_f = \tfrac{1}{2}\left(\sqrt{D^2 + 4\nu(\nu-1)} - D\right), \tag{14}$$

are integer numbers for different values of ν.The ψ_S factor ensures that the wave function (12) is totally antisymmetric with respect to the interchange of particles. For $D = 2$ there are two such determinants that are linearly independent and can be chosen such that they are both eigenfunctions of the angular-momentum operator:

$$\psi_S^\pm = \begin{cases} (x_1 - x_2) + i(y_1 - y_2) \\ (x_1 - x_2) - i(y_1 - y_2) \end{cases} \quad L_z\psi_S^\pm = \pm\psi_S^\pm. \tag{15}$$

Ground-state wave functions can be constructed by using linear combinations of $\psi_S^\pm$, but this does not imply that their corresponding reduced density matrices have the same entanglement entropies, as we show in the following sections.

III. NATURAL OCCUPATION NUMBERS AND VON NEUMANN ENTROPY: ONE-DIMENSIONAL CASE

The one-dimensional case was thoroughly analyzed in Ref. [4] for those values of ν that are compatible with an exact calculation of the p-RDM and its eigenvalues, i.e., for $\nu = 2n$ (bosons) and $\nu = 2n+1$ (fermions), with n a natural number.

In the present work we consider ν as a continuous variable and calculate by using the Rayleigh–Ritz variational method, the eigenvalues of the reduced density matrix (2). How to use the variational method to calculate an approximate spectrum

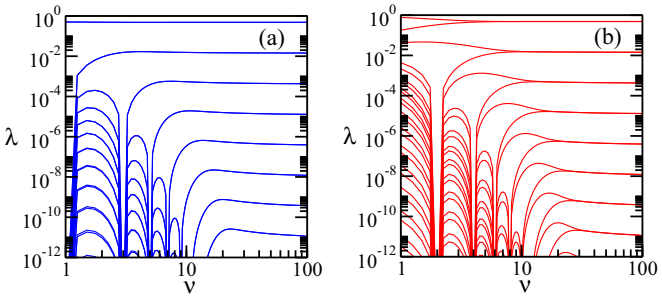

FIG. 1. Eigenvalues of the 1-RDM for the ground state of a one-dimensional Calogero model from a variational calculation, using 50 one-particle basis functions. Panel (a) shows the results for fermions and panel (b) shows those for bosons. The abrupt drop to zero of the eigenvalues at certain integer values (odd for fermions, even for bosons) indicate that the number of natural orbitals is finite. In panel (a), each eigenvalue is doubly degenerate.

for a reduced density matrix has been described elsewhere—see Refs. [21,23,32]. The natural choice of basis set is the Hermite functions used to obtain the exact eigenvalues of the finite 1-RDM matrix for integer values of ν [4].

The eigenvalues calculated by using the variational method for bosons and fermions are shown in a log - log plot in Fig. 1. The most salient feature of both sets of curves is the abrupt way in which most eigenvalues drop to zero at the integer values of ν (see Sec. II).

In the fermion case, since all the eigenvalues are doubly degenerate [33], there are only four eigenvalues—the larger ones—that never become null. For $\nu = 2n + 1$, there are only $2n + 2$ nonzero eigenvalues [4]. The numerical error of the variational eigenvalues for integer values of ν is $O(\epsilon_m)$ where $\epsilon_m \approx 2 \times 10^{-15}$ is the machine precision.

For large values of the interaction parameter $\nu(\nu - 1)$, the NONs of bosons and fermions become equal, as can be seen in Fig. 2(a). As a consequence, the von Neumann entropy for both statistics turns out to be the same in the large-interaction limit—see Fig. 2(b). It is important to mention that, in this limit, vNE converges to a finite value that can be calculated analytically [4,34].

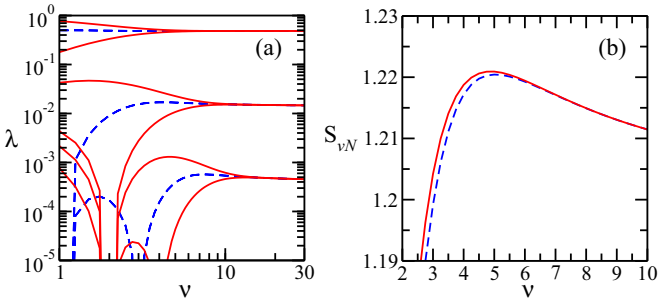

FIG. 2. (a) Bosons (red line) and fermions (blue dashed line) larger eigenvalues of the 1-RDM and (b) von Neumann entropy for the two-particle ground state of a one-dimensional Calogero model from a variational calculation using 50 one-particle basis functions. Note that the eigenvalues of fermions and bosons become degenerate in the large-interaction limit.

As can be seen in Fig. 2(b), the vNE shows a maximum around $\nu = 5$ for both cases. The appearance of a maximum in the vNE is, at some extent, unexpected since in systems with continuous variables the vNE is known to have a behavior that is strongly correlated to the derivative of the energy with respect to the interaction parameter (see, for example, Refs. [32,35]). For bound states, it is observed that the vNE increases when the derivative of the energy with respect to the interaction strength diminishes. In our case the derivative increases monotonically but the vNE is not a monotonic function, in contradistinction with what is observed in three-dimensional atom-like systems.

Usually, a nonmonotonic behavior of an information-content quantifier, as an entanglement measure or an entropy, is related to changes in the analyticity of the ground-state energy, as happens in a quantum phase transition [36]. Another reason might be changes in the relative weight between states with different entanglement as happens when the temperature is varied in some thermal mixes [37]. The ground-state energy and totally symmetric or antisymmetric wave function Eqs. (8) and (10) are analytical with respect to the parameter ν. Moreover, the 1-RDM eigenvalues, which are directly related to the vNE, are shown to be analytical around integer ν by using the variational eigenvalues and finite-size scaling for quantum mechanics techniques (see Supplemental Material [38]).

IV. RÉNYI ENTROPIES AND FINITE SUPPORT OF THE REDUCED DENSITY MATRICES

The smooth behavior of the von Neumann entropy fails to manifest the structure of the 1-RDM spectrum as a function of the strength parameter ν. No relevant features are observed at the isolated values of ν for which the 1-RDM has only a finite set of nonzero eigenvalues and the support of the 1-RDM becomes finite, i.e., the Hilbert space where the system is described becomes finite. As we will show below, the smooth behavior is imposed by the analyticity of the eigenvalues with ν.

Nevertheless, the structure of the spectrum can be put in evidence by the Rényi entropies, defined in Eq. (4). As has been pointed out the Rényi entropies allow us to probe different regions of the spectrum because changing α assigns different weights to the eigenvalues.

The eigenvalues of the 1-RDM are analytical functions of ν (see Supplemental Material [38]). We develop here the boson case (the fermion case is similar) for $\nu_n = 2n$, where the 1-RDM has only $2n + 1$ nonzero eigenvalues.

The following results will only rely on the analyticity of the eigenvalues around isolated points in the parameter space where the spectrum is finite. As such, they will be valid for any system having this property. We then assume

$$\lambda_i(\nu) \sim \begin{cases} \lambda_i(\nu_n) + \lambda_i^{(1)}(\nu - \nu_n) & \text{if } i \leqslant 2n+1 \\ \lambda_i^{(2)}(\nu - \nu_n)^{2k_{i,n}} & \text{if } i > 2n+1, \end{cases} \quad \text{for } \nu \to \nu_n \tag{16}$$

where $\lambda_i^{(1)},\lambda_i^{(2)}$ are constants, and $k_{i,n} \geqslant 1$ is an integer. Equation (4) can be written as

$$\begin{aligned} S^\alpha(\nu) &= \frac{1}{1-\alpha}\log_2\left(\sum_{i=1}^{2n+1}\lambda_i^\alpha(\nu)+\sum_{i=2n+2}^{\infty}\lambda_i^\alpha(\nu)\right) \\ &= \frac{1}{1-\alpha}\left[\log_2\left(\sum_{i=1}^{2n+1}\lambda_i^\alpha(\nu)\right)\right. \\ &\quad \left.+\log_2\left(1+\frac{\sum_{i=2n+2}^{\infty}\lambda_i^\alpha(\nu)}{\sum_{i=1}^{2n+1}\lambda_i^\alpha(\nu)}\right)\right] \\ &\underset{\nu\to\nu_n}{\sim} \frac{1}{1-\alpha}\left[\log_2\left(\sum_{i=1}^{2n+1}\lambda_i^\alpha(\nu)\right)+\frac{\sum_{i=2n+2}^{\infty}\lambda_i^\alpha(\nu)}{\ln 2\sum_{i=1}^{2n+1}\lambda_i^\alpha(\nu)}\right] \\ &= S_n^\alpha(\nu)+s_n^\alpha(\nu). \end{aligned} \tag{17}$$

Note that $S_n^\alpha(\nu_n)=S^\alpha(\nu_n)$, and $s_n^\alpha(\nu_n)=0$. We can evaluate the derivative of the Rényi entropy at $\nu=\nu_n$,

$$\begin{aligned} &\left.\frac{\partial S^\alpha(\nu)}{\partial\nu}\right|_{\nu=\nu_n} \\ &= \left.\frac{\partial S_n^\alpha(\nu)}{\partial\nu}\right|_{\nu=\nu_n}+\frac{\alpha}{\ln 2(1-\alpha)}\left(\frac{\sum_{i=2n+2}^{\infty}\lambda_i^{\alpha-1}(\nu)\partial_\nu\lambda_i(\nu)}{\sum_{i=1}^{2n+1}\lambda_i^\alpha(\nu)}\right. \\ &\quad \left.-\frac{\sum_{i=2n+2}^{\infty}\lambda_i^\alpha(\nu)\sum_{i=1}^{2n+1}\lambda_i^{\alpha-1}(\nu)\partial_\nu\lambda_i(\nu)}{\left(\sum_{i=1}^{2n+1}\lambda_i^\alpha(\nu)\right)^2}\right)_{\nu=\nu_n}. \end{aligned} \tag{18}$$

The first term in Eq. (18) is a well-defined constant and the third one is zero. As a result of this, the derivative is dominated by the second term. By using the analytic expansion of the eigenvalues, Eq. (16), and assuming that k_m is the minimum value of $k_{i,n}$, the leading asymptotic behavior of s_n^α is

$$s_n^\alpha(\nu)\underset{\nu\to\nu_n}{\sim} C_n[(\nu-\nu_n)^{2k_m}]^\alpha = C_n|\nu-\nu_n|^{\delta k_m}, \tag{19}$$

where $\delta=2\alpha$, which implies that

$$\frac{\partial s_n^\alpha(\nu)}{\partial\nu}\underset{\nu\to\nu_n}{\sim}\delta k_m C_n|\nu-\nu_n|^{\delta k_m-1}\mathrm{sign}(\nu-\nu_n). \tag{20}$$

This equation gives

$$\begin{aligned} &\left.\frac{\partial S^\alpha(\nu)}{\partial\nu}\right|_{\nu=\nu_n} \\ &= \begin{cases} \left.\begin{array}{ll} -\mathrm{sign}(C_n)\times\infty & \text{for } \nu\to\nu_n^- \\ \mathrm{sign}(C_n)\times\infty & \text{for } \nu\to\nu_n^+ \end{array}\right\} & \text{if } k_m\delta<1 \\ \left.\begin{array}{ll} \partial_\nu S_n^\alpha(\nu_n)-C & \text{for } \nu\to\nu_n^- \\ \partial_\nu S_n^\alpha(\nu_n)+C & \text{for } \nu\to\nu_n^+ \end{array}\right\} & \text{if } k_m\delta=1 \\ \partial_\nu S_n^\alpha(\nu_n) & \text{if } k_m\delta\geqslant 1. \end{cases} \end{aligned} \tag{21}$$

Even though the derivative of S^α is continuous for $k_m\delta\geqslant 1$, it is straightforward to see from the eigenvalue asymptotics, Eq. (16), that the second derivative diverges for $1<k_m\delta<2$ but is analytical for $k_m\delta=2$, i.e., the kink at $k_m\delta=1$ is smoothed until it disappears at $k_m\delta=2$.

All our numerical evidence indicates that, in the case of the one-dimensional Calogero model, $k_m=1$ for all values of i and n (see Supplemental Material [38]). The Rényi entropy will then present critical points with infinite derivative for $\alpha<1/2$, a kink for $\alpha=1/2$ which continuously disappears for increasing α until the value 1 is reached. The vNE which can be obtained as the Rényi entropy with $\alpha\to 1$ is then an analytical function of ν.

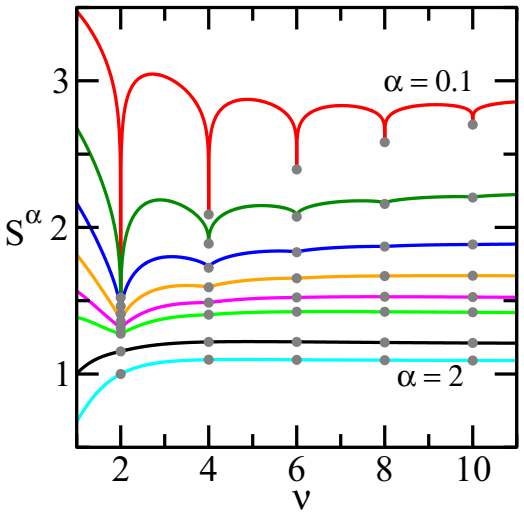

FIG. 3. One-dimensional bosonic von Neumann entropy (black full line) and Rényi entropies as a function of the interaction parameter ν, for $\alpha=0.1, 0.2, 0.3, 0.4, 0.5, 0.6, 2$ in red, dark green, blue, orange, magenta, light green, and cyan full line, respectively. The exact values of the entropies for $\nu=2n$ are depicted as gray points.

The nonanalytical behavior of the Rényi entropies predicted by Eq. (21) are a consequence of the eigenvalues analyticity assumption; Eq. (16). This salient feature is easily recognizable for $\nu=2n$ in Fig. 3, where the variational Rényi entropies for the one-dimensional bosonic Calogero system are shown as a function of the interaction strength parameter for several values of α. This figure also shows the exact Rényi entropies for those values of ν for which the 1-RDM has finite support, $\nu=2n$. It is worth mentioning that the Rényi entropies are decreasing functions of α, so the top curve being plotted corresponds to the smaller value chosen for α, and that they are bounded from below by the one-dimensional min-entropy S_x^∞ value [see Eq. (51)].

The Rényi entropy and its derivative as a function of the interaction-strength parameter near $\nu=4$ are depicted for $\alpha=0.4, 0.5, 0.6$ in Fig. 4. The figure supports all the predictions described above. It shows that the Rényi entropy presents a critical point with infinite derivative for $\alpha=0.4$, a kink with discontinuous derivative for $\alpha=1/2$ and a continuous derivative for $\alpha=0.6$ with an infinite second derivative.

Summarizing, the Rényi entropies expose the values of ν which give a 1-RDM with finite support and this makes them excellent witnesses to detect such a hallmark. Similar features were also seen by Amico and coworkers for spin-1/2 chains [39–42].

V. NATURAL OCCUPATION NUMBERS AND VON NEUMANN ENTROPY: TWO-DIMENSIONAL CASE

The wave function of the two-particle two-dimensional Calogero model is known for all values of ν [see Eqs. (11)

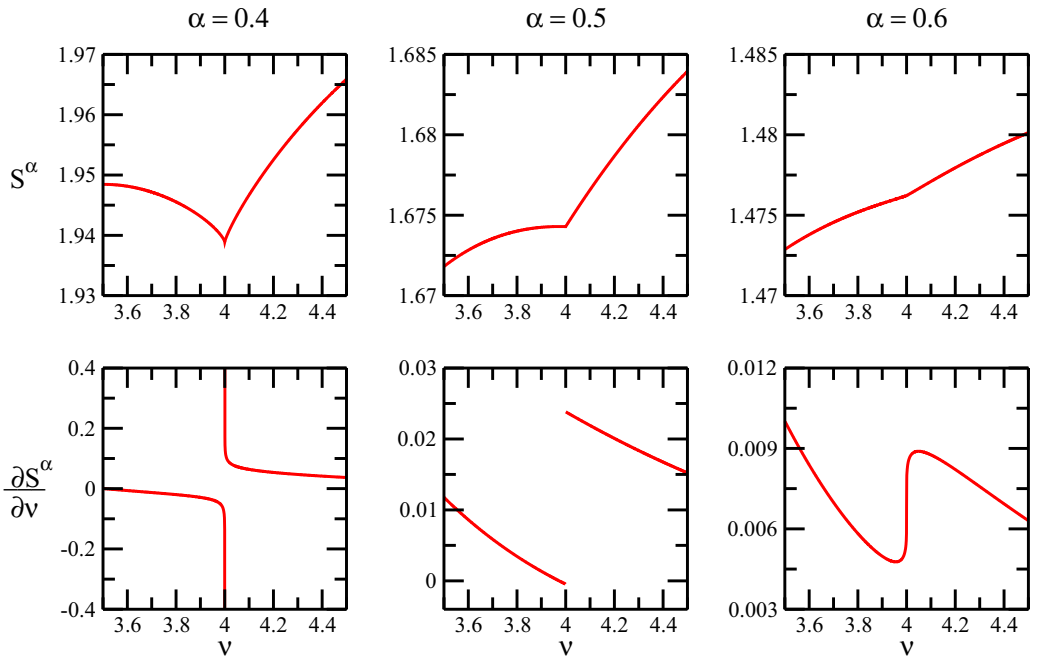

FIG. 4. One-dimensional bosonic Rényi entropies (upper panels) and their derivatives (lower panels) as a function of the interaction parameter near $\nu = 4$, for $\alpha = 0.4, 0.5, 0.6$ from top to bottom.

and (12)]. On the other hand, the 1-RDM, its eigenvalues, and other related quantities are obtained numerically by means of the Rayleigh–Ritz variational method. The behavior of the vNE is shown in Fig. 5(a) for the boson and fermion cases. In this figure, the continuous red line corresponds to the boson case, and the dashed lines correspond to fermions. The green dashed line corresponds to $\psi_S = \psi_S^+ = (x_1 - x_2) + i(y_1 - y_2)$, while the blue dashed line corresponds to $\psi_S = \psi_S^x = \frac{1}{\sqrt{2}}(\psi_S^+ + \psi_S^-)$. From the obtained lines in a log scale it can be seen that the three sets of data are consistent with a logarithmic divergence of the vNE when the parameter ν increases, as we explain in the next section.

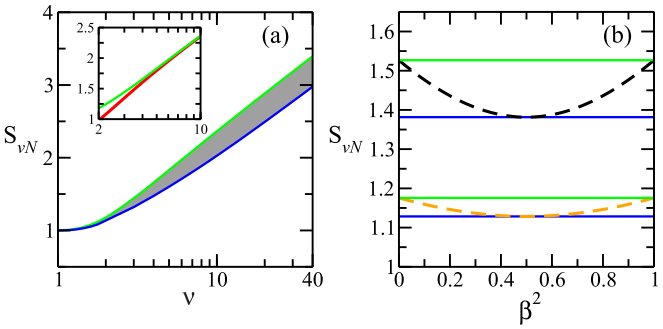

FIG. 5. (a) The von Neumann entropy as a function of the interaction strength ν for the rotationally invariant fermion wave function ψ_S^+ (green line) and for the fermion wave function $\psi_S^x = (x_1 - x_2)$ (blue line). Note the logarithmic divergence for large interaction strength. Any point in the gray shaded area is a (ν, S_{vN}) pair, which can be obtained from a particular choice of the linear combination parameter β defined in Eq. (23). The inset shows that the vNE for the rotationally-invariant-fermion case (green line) is asymptotically equal to the vNE for bosons (red line). (b) The fermion vNE of $\psi_{lc}(\beta)$ as a function of β^2 across the shaded region for two values of the interacting parameter, $\nu = 2$ (orange-dashed line) and $\nu = (1 + \sqrt{33})/2$ (black-dashed line). The horizontal lines correspond to the vNE of ψ_S^+, ψ_S^x.

With the above definition of ψ_S^x and by defining $\psi_S^y = \frac{1}{\sqrt{2}}(\psi_S^+ - \psi_S^-)$, one can construct the related fermion ground-state functions Ψ_0^{f+}, Ψ_0^{f-}, Ψ_0^{fx}, and Ψ_0^{fy} by substituting ψ_S^+, ψ_S^-, ψ_S^x, and ψ_S^y in Eq. (12). It can then be shown that

$$\begin{aligned}\left|\Psi_0^b[\nu(\nu-1)+1]\right|^2 &= \left|\Psi_0^{f\pm}[\nu(\nu-1)]\right|^2 \\ &= \tfrac{1}{2}\left|\Psi_0^{fx}[\nu(\nu-1)]\right|^2 \\ &\quad + \tfrac{1}{2}\left|\Psi_0^{fy}[\nu(\nu-1)]\right|^2, \end{aligned} \tag{22}$$

where the argument between square brackets is the interaction strength in Eq. (6) for which the ground-state function must be calculated.

The first two terms in the equality obtained ensures that, for large enough values of ν, the von Neumann entropies for bosons and fermions are asymptotically the same if the corresponding states are eigenfunctions of L_z. So far, we have not found how to translate the relationship between the square modulus of the wave functions in Eq. (22) to a relationship between the NONs of their respective 1-RDM.

The availability of degenerate fermion ground-state functions allows us to study the von Neumann entropy for different linear combinations of orthogonal states. In particular, we studied the vNE of different ground-state wave functions obtained by replacing ψ_S in Eq. (12) with the following expression:

$$\psi_{lc}(\beta) = \beta\psi_S^+ + \sqrt{1-\beta^2}\psi_S^-, \quad \beta \in [0,1]. \tag{23}$$

The vNEs for the previously defined states, $\psi_{lc}(\beta)$, ψ_S^x, and Ψ_0^b, are shown in Fig. 5. There is a number of interesting features in Fig. 5(a) which are noteworthy. The vNEs for all the states defined by Eq. (23) diverge logarithmically in the large-interaction-strength limit. For a given ν value, the entropies of $\psi_S^{\pm}$ ($\beta = 0$, $\beta = 1$) are maximal while those of $\psi_S^{x,y}$ ($\beta = \pm\frac{1}{\sqrt{2}}$) are minimal over $S_{vN}[\psi_{lc}(\beta)]$, the shaded region corresponds to all other possible values of β. Also, in the large-interaction-strength limit, the vNEs of both fermion states $\psi_S^{\pm}$ and the boson ground state are asymptotically equal [see the inset in Fig. 5(a)]. Figure 5(b) shows the behavior of the vNE calculated for the ground states constructed by using Eq. (23) as a function of β^2, for $\nu = 2$ (numerical) and for $\mu_f = 2 \Rightarrow \nu = (1+\sqrt{33})/2$ (exact).

The linear entropy shows a different behavior; it converges monotonically to unity in the large-interaction-strength limit. This behavior has been reported previously for a number of systems and is usually associated with the competing nature of the potentials in the Hamiltonian [22,43]; for example, in Eqs. (6) and (7) the harmonic term keeps the particles near the origin of coordinates, while the repulsive term tries to keep them as far as possible, especially when $\nu \to \infty$.

Logarithmic divergences are always elusive to pinpoint when based only in numerical data. The reason is that it is quite cumbersome to study large values of ν because of the huge number of base functions needed (that scales as ν^2) to put in evidence the logarithmic divergence. Nevertheless, we have been able to obtain the vNE for values up to $\nu = 80$. To support the numerical evidence shown in Fig. 5 we then proceed to study an analytical approximation to the two-dimensional problem.

VI. ANALYTICAL TREATMENT OF ANISOTROPIC TWO-DIMENSIONAL CALOGERO MODEL IN LARGE-INTERACTION-STRENGTH LIMIT

The argument stated some paragraphs above about the competing nature of the potentials involved in the Calogero model has been useful to develop a method dedicated to obtain analytical approximations to the eigenfunctions and eigenvalues of Hamiltonians. The method is based on the calculation of the minima of the potential and the harmonic approximation consistent with those minima [34,44]. Of course for two- or three-dimensional problems those minima are not necessarily given by a set of isolated points. There is a rather simple way to circumvent the arising difficulties when the minima set is not discrete: the potential is "deformed" to obtain a finite number of minima [43]. The deformation breaks the symmetry between the coordinates. For example, in the two-dimensional Hamiltonian, we can take $y_i \mapsto \varepsilon y_i$. Within this framework it is possible to study the two-dimensional isotropic system as a limiting case of the deformed one' therefore, we consider a two-dimensional anisotropic Calogero model

$$H = -\frac{1}{2}\left(\nabla_1^2 + \nabla_2^2\right) + \frac{1}{2}\left\{\left(x_1^2 + x_2^2\right) + \varepsilon^2\left(y_1^2 + y_2^2\right)\right\} + \frac{\nu(\nu-1)}{r_{12}^2}. \tag{24}$$

Introducing the center of mass $\vec{R} = \frac{1}{2}(\vec{x}_1 + \vec{x}_2) = (X,Y)$ and relative coordinates $\vec{r} = \vec{x}_2 - \vec{x}_1 = (x,y)$, the Hamiltonian (24) may be written as $H = H^R + H^r$, where

$$H^R = -\tfrac{1}{4}\nabla_R^2 + (X^2 + \varepsilon^2 Y^2), \tag{25}$$

$$H^r = -\nabla_r^2 + \frac{1}{4}(x^2 + \varepsilon^2 y^2 + \frac{\nu(\nu-1)}{(x^2+y^2)}. \tag{26}$$

The wave function is then the product of the center-of-mass (CM) wave function and the relative wave function $\Psi(X,Y,x,y) = \psi^R(X,Y)\psi^r(x,y)$, and the Schrödinger equation separates into two equations:

$$H^R\psi^R(\vec{R}) = E^R\psi^R(\vec{R}), \tag{27}$$

$$H^r\psi^r(\vec{r}\,) = E^r\psi^r(\vec{r}\,). \tag{28}$$

The solutions of the CM Eq. (27) have the following form:

$$\psi^R_{n,m}(\vec{R}) = e^{-X^2}H_n(\sqrt{2}X)e^{-\varepsilon Y^2}H_m(\sqrt{2\varepsilon}Y), \tag{29}$$

with energies

$$E^R_{n,m} = \left(n + \tfrac{1}{2}\right) + \varepsilon\left(m + \tfrac{1}{2}\right). \tag{30}$$

With the aim of solving the relative Schrödinger equation (28) in the large-interaction-strength limit we use the harmonic approximation (HA) [44,45]. The classical minima of the potential terms are given by $\vec{r}_{\min} = (\pm\sqrt{2}[\nu(\nu-1)]^{\frac{1}{4}},0)$. In this approximation the Hamiltonian is

$$H^r_{HA} = -\nabla_r^2 + \tfrac{1}{2}\left\{2(x-x_0)^2 + \tfrac{1}{2}(\varepsilon^2-1)y^2\right\}, \tag{31}$$

where $x_0 = \sqrt{2}[\nu(\nu-1)]^{\frac{1}{4}}$.

The solutions to Eq. (28) are

$$\psi^r_{n,m}(\vec{r}) = e^{-\frac{(x-x_0)^2}{2}}H_n(x-x_0)e^{-\frac{\sqrt{\varepsilon^2-1}}{4}y^2}H_m\left[\left(\frac{\varepsilon^2-1}{4}\right)^{1/4}y\right], \tag{32}$$

with eigenvalues

$$E^r_{n,m} = 2\left(n + \tfrac{1}{2}\right) + \sqrt{\varepsilon^2-1}\left(m + \tfrac{1}{2}\right). \tag{33}$$

From Eqs. (29) and (32), the total normalized symmetric ground-state wave function can be obtained,

$$\Psi(\vec{r}_1,\vec{r}_2) = Ce^{-\varepsilon\frac{(y_1+y_2)^2}{4}}e^{-\sqrt{\varepsilon^2-1}\frac{(y_2-y_1)^2}{4}}e^{-\frac{(\tilde{x}_1+\tilde{x}_2)^2}{4}}\left\{e^{-\frac{(\tilde{x}_2-\tilde{x}_1)^2}{2}} + e^{-\frac{(\tilde{x}_1-\tilde{x}_2)^2}{2}}\right\}, \tag{34}$$

where $\tilde{x}_1 = x_1 + \frac{x_0}{2}$ and $\tilde{x}_2 = x_2 - \frac{x_0}{2}$, and the normalization constant

$$C = \left(\frac{\sqrt{\varepsilon\sqrt{\varepsilon^2-1}}}{\sqrt{2}\pi^2(1+e^{-2\sqrt{\nu(\nu-1)}})}\right)^{\frac{1}{2}}. \tag{35}$$

The wave function (34) is separable in the x and y coordinates and can be written as $\Psi(\vec{r}_1,\vec{r}_2) = C\psi_x(\tilde{x}_1,\tilde{x}_2)\psi_y(y_1,y_2)$.

Since we are interested in the occupancies of the natural orbitals, we must solve the integral equation (2). The iterated kernel of a symmetric kernel has the same eigenfunctions as the kernel, and the iterated eigenvalues are the squared eigenvalues

of the kernel [21,46], that is, instead of solving Eq. (2) one can solve

$$\int \Psi(\vec{r}_1,\vec{r}_2)\phi_k(\vec{r}_2)d\vec{r}_2 = \ell_k\phi_k(\vec{r}_1). \tag{36}$$

The solution to this eigenvalue problem is equivalent to find the Schmidt decomposition of the functions $\psi_x(\tilde{x}_1,\tilde{x}_2)$ and $\psi_y(y_1,y_2)$ given by

$$\psi_x(\tilde{x}_1,\tilde{x}_2) = q(\tilde{x}_1,\tilde{x}_2) + q(\tilde{x}_2,\tilde{x}_1), \tag{37}$$

where

$$q(\tilde{x}_1,\tilde{x}_2) = e^{-\frac{3}{4}(\tilde{x}_1^2+\tilde{x}_2^2)+\frac{1}{2}\tilde{x}_1\tilde{x}_2}, \tag{38}$$

and

$$\psi_y(y_1,y_2) = e^{-\frac{\varepsilon+\sqrt{\varepsilon^2-1}}{4}(y_1^2+y_2^2)-\frac{\varepsilon-\sqrt{\varepsilon^2-1}}{2}y_1y_2}. \tag{39}$$

By using Mehler's formula

$$e^{-(u^2+v^2)\frac{y^2}{1-y^2}+uv\frac{2y}{1-y^2}} = \sum_{k=0}^{\infty}\sqrt{1-y^2}\left(\frac{y}{2}\right)\frac{H_k(u)H_k(v)}{k!}, \tag{40}$$

it is possible to find the decomposition of Eqs. (38) and (39),

$$\psi(u,v) = \sum_{k=0}^{\infty}\ell_k\phi_k(u)\phi_k(v). \tag{41}$$

After performing some algebra one gets the eigenvalues of the 1-RDM in the limit of large interaction-strength parameter ν,

$$\lambda_{k,k'} = 2\left(3\sqrt{2}-4\right)[1-\xi(\varepsilon)]\xi(\varepsilon)^k\left(17-12\sqrt{2}\right)^{k'}, \tag{42}$$

where

$$\xi(\varepsilon) = \left(\frac{(\varepsilon^2-1)^{\frac{1}{4}}-\sqrt{\varepsilon}}{(\varepsilon^2-1)^{\frac{1}{4}}+\sqrt{\varepsilon}}\right)^2. \tag{43}$$

Knowing the eigenvalues it is easy to calculate the LE (5):

$$S_{le} = 1-\left(\frac{3\sqrt{2}-4}{9-6\sqrt{2}}\right)\frac{1-\xi(\varepsilon)}{1+\xi(\varepsilon)}. \tag{44}$$

Since the wave function is separable, the von Neumann entropy presents the form

$$S_{vN} = S^x + S^y(\varepsilon), \tag{45}$$

where each one of the terms in the sum has the form of the one-dimensional vNE [34], i.e.,

$$S^x = 1.197\,371\,889, \tag{46}$$

$$S^y(\varepsilon) = -\frac{\ln\left([1-\xi(\varepsilon)]^{2[1-\xi(\varepsilon)]}\xi(\varepsilon)^{2\xi(\varepsilon)}\right)}{\ln(4)[1-\xi(\varepsilon)]}. \tag{47}$$

The Rényi entropy Eq. (4) in the large interaction limit can be written as

$$S^\alpha = S_x^\alpha + S_y^\alpha, \tag{48}$$

where

$$S_x^\alpha = \frac{1}{1-\alpha}\log_2\left(\frac{(6\sqrt{2}-8)^\alpha}{[1-(17-12\sqrt{2})^\alpha]}\right)+1, \tag{49}$$

and

$$S_y^\alpha = \frac{1}{1-\alpha}\log_2\left(\frac{[1-\xi(\varepsilon)]^\alpha}{[1-\xi(\varepsilon)^\alpha]}\right). \tag{50}$$

The isotropic model can be recovered taking $\varepsilon \to 1^+$. In this limit $\xi(\varepsilon)\to 1$, all the eigenvalues go to zero and the vNE diverges logarithmically while the LE goes to one. For any other values of ε the vNE is finite and the LE remains below one. It is important to emphasize that the previous analysis can be generalized to dimension D, deforming the isotropic potential in $D-1$ dimensions. The one-dimensional problem is recovered for large anisotropy parameter, $\varepsilon \gg 1$, case in which $\xi(\varepsilon)\to 0$ and consequently $S_{le}\to 1-\frac{\sqrt{2}}{3}$ and $S_{vN}\to S^x$.

The Rényi entropy as a function of the anisotropy parameter shows the same behavior as the vNE: it diverges logarithmically for $\varepsilon\to 1^+$ and for $\varepsilon \gg 1$ it reaches the one-dimensional value S_x^α. It is worth noticing that, from Eq. (49), it is straightforward to demonstrate that the one-dimensional min-entropy S_x^∞ has the following form:

$$S_x^\infty = \lim_{\alpha\to\infty} S_x^\alpha = \log_2\left(1+\frac{3}{2\sqrt{2}}\right). \tag{51}$$

VII. TWO- TO ONE-DIMENSIONAL CROSSOVER

As pointed out in Sec. VI, the one-dimensional vNE and LE in the large-interaction-strength limit are exactly recovered from the two-dimensional model harmonic approximation for large anisotropy parameter. This immediately raises the question of how the two- to one-dimensional *crossover* is manifested in the entropies and whether there is also a similar feature for finite values of the interaction parameter ν. Let us first look at the large-interaction limit and then compare it to the numerical results for finite ν.

The exact vNE of the anisotropic two-dimensional harmonic approximation [Eq. (45)] is depicted in magenta dot-dashed line in Fig. 6. Albeit there is not a clear-cut criterion to detect the change from two- to one-dimensional behavior, or crossover, one can notice that the one-dimensional limit is reached for $\varepsilon \gtrsim 1.5$. Moreover, the vNE is finite for any value of $\varepsilon > 1$ as it is in the one-dimensional case.

Calculating the first derivative of Eq. (47) it is straightforward to demonstrate that

$$S_{vN} \sim -\frac{\log(\varepsilon-1)}{\log 16} \text{ for } \varepsilon\sim 1^+, \tag{52}$$

this behavior is depicted in Fig. 6 as a yellow dashed line which makes the logarithmic divergence of the vNE for $\varepsilon\to 1^+$ evident.

The entropies obtained by adding up the contributions of a finite number of exact eigenvalues [Eq. (42)] are also shown in Fig. 6. The plot reveals that, no matter how many eigenvalues are used to evaluate the vNE, there is always a value of ε for which the vNE reaches a maximum and decays for smaller values of the parameter. In other words, the more isotropic the system is, the larger the number of NONs that are needed to correctly describe the problem. This is precisely the reason that makes the identification of a logarithmic divergence so difficult, since using a finite numerical approach only provides a finite number of approximate eigenvalues to calculate the vNE.

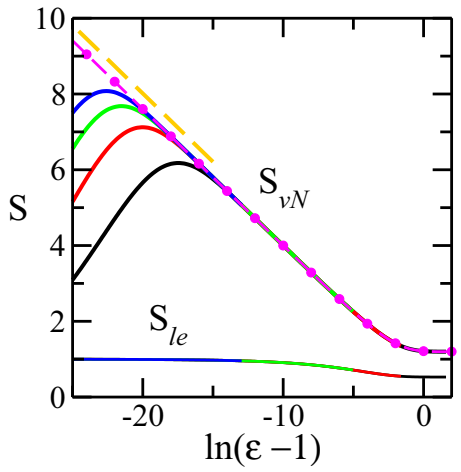

FIG. 6. von Neumann (vNE) and linear entropy (LE) in the large-interaction limit computed by using finite sums of the exact eigenvalues (full lines) and the exact vNE (magenta dot-dashed line) as a function of the anisotropy parameter ε [Eq. (45)]. The number of included eigenvalues [Eq. (42)] are 50 (black), 100 (red), 150 (green), and 200 (blue) respectively. The leading term of the exact vNE, Eq. (52), is depicted as a yellow dashed line (shifted to make it visible).

Let us now compare the harmonic approximation to the finite-interaction-strength results. In Sec. V we argued that the vNE shown in Fig. 5(a) grows logarithmically. The divergence for $\varepsilon \to 1^+$ in the large interaction limit proves that *the vNE of the isotropic Calogero model is infinite* and reinforces what was numerically inferred: the growth is sustained and it is a logarithmic divergence.

More evidence of the convergence of the finite-ν behavior to the one observed in the isotropic harmonic approximation can be obtained by studying the ground-state energy of the deformed Hamiltonian. The eigenvalues of the relative Hamiltonian, Eq. (33), depend in a nonanalytical fashion on the deformation parameter in the large-interaction limit. We will then compare the ground-state energy of the harmonic approximation $[E^r_{00}(\varepsilon)]$ to the one obtained from a variational approach in Hamiltonian (26) for finite ν at different anisotropies parameter ε $[E^{\rm var}_{00}(\nu,\varepsilon)]$. We define E^{∞}_{00} as

$$E^{\infty}_{00}(\nu,\varepsilon) = \frac{E^{\rm var}_{00}(\nu,\varepsilon)}{E^r_{00}(\varepsilon) - 1}. \tag{53}$$

Figure 7(a) shows how $E^{\infty}_{00}(\nu,\varepsilon)$ approaches the nonanalytical behavior of the function $(\varepsilon^2-1)^{1/2}$ for large enough values of ν. Notice that, for large enough anisotropy ε, the system, no matter how small the interaction strength ν is, reaches the one-dimensional limit. This observation implies that an anisotropic system should behave as a two-dimensional or one-dimensional one depending on the interplay between the parameters ν and ε.

Another quantity that also shows the crossover can be defined as

$$\Delta E^{\rm var}_{00}(\varepsilon) = \sqrt{\varepsilon^2-1}\left(\frac{E^{\rm var}_{00}(\varepsilon+\Delta\varepsilon) - E^{\rm var}_{00}(\varepsilon-\Delta\varepsilon)}{2\Delta\varepsilon}\right), \tag{54}$$

and is displayed in Fig. 7(b). Due to the dependence of the relative ground-state energy, in the large-interaction-strength limit, the following relationship is satisfied:

$$\sqrt{\varepsilon^2-1}\frac{dE^r_{00}}{d\varepsilon} = \frac{\varepsilon}{2}. \tag{55}$$

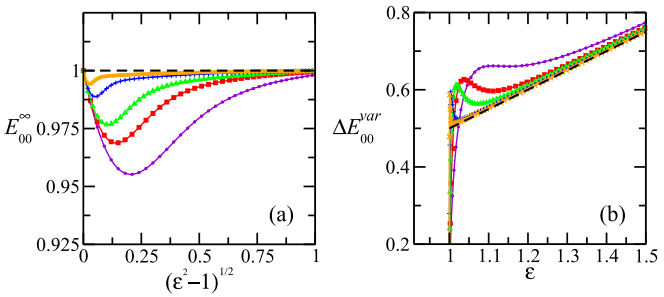

FIG. 7. (a) The data corresponds to the ratio between the variational energy and the energy of the relative Hamiltonian in the large-interaction limit, E^{∞}_{00} [see Eq. (53)]. The variational energies were calculated for, from bottom to top, $\nu(\nu-1) = 20, 50, 100, 500, 2000$. The black dashed line corresponds to the exact limit. (b) The numerical derivative of the variational ground-state energy times $(\varepsilon^2-1)^{1/2}$ vs ε; see Eq. (55) for the precise definition of the function $\Delta E^{\rm var}_{00}$. This function was chosen to show the derivative of the ground-state energy of the relative Hamiltonian in the limit $\nu \to \infty$ as the black dashed straight line with slope one-half. The other curves correspond to the data shown in panel (a) using the same color convention for the different values of $\nu(\nu-1)$.

Figure 7(b) shows how the variational data, Eq. (54), approaches a straight line with slope one-half, which corresponds to the large-interaction limit in Eq. (55).

Summarizing, all the previous analyses indicate a two- to one-dimensional crossover. Moreover, the vNE diverges logarithmically for the two-dimensional isotropic system, while it remains finite in the anisotropic cases.

VIII. DISCUSSION AND CONCLUSIONS

In the present work, we study the von Neumann and Rényi entropies for the two-particle one- and two-dimensional Calogero model. We found that the von Neumann entropy of the two-dimensional model with isotropic confinement is a monotonic increasing function of the interaction strength that diverges logarithmically for large-interaction-strength values, while it remains finite in the anisotropic case as well as in the one-dimensional model. We also show that the one-dimensional behavior is eventually reached when the anisotropy of a two-dimensional system is increased. By using the framework of the harmonic approximation, the crossover from two to one dimensions is demonstrated, and it is shown that the von Neumann divergence only occurs in the isotropic case.

On the other hand, we found that the Rényi entropies expose those values of ν which give a one-particle reduced density matrix with finite support. Amico and coworkers have found nonanalytical behavior for spin-1/2 chains at the critical values of the Hamiltonian interaction parameters [39–42].

Let us now discuss the physical implications of the results summarized above. The logarithmic divergence of the von Neumann entropy of the two-dimensional Calogero model is, somewhat, to be expected, since the von Neumann entropy

of the Laughlin wave function diverges for decreasing filling factors [25]. However, the connection is not direct since the bipartition considered in the work of Iblisdir *et al.* [25] differs from the one chosen in the present work. Even more, the three-dimensional continuous variable systems studied in the literature support the idea that, if the ground-state energy of the Hamiltonian is an analytical and monotonic function of some interaction parameter, so is the von Neumann entropy. These arguments highlight the singularity of the one-dimensional case.

The fact that an anisotropic two-dimensional case behaves like a one-dimensional system, in what concerns its von Neumann entropy, supports the idea that the nonmonotonic behavior is owed to the restriction of the problem to a "truncated" Hilbert space.

In the same sense, the Rényi entropies for small-enough α have a nonmonotonic and nonanalytical behavior in the neighborhood of the interaction-strength-parameter values where the support of the reduced density matrix is finite. It is important to emphasize that *the deduction of the nonanalytical behavior of the derivatives of the Rényi entropies is completely general*, the only features that are unique to the Calogero model are that the values of ν where the 1-RDM has a finite entanglement spectrum and the number of nonzero eigenvalues for each one are exactly known. Consequently, the Rényi entropies seems to be a handy tool to detect parameters where a given system possess an exact and finite entanglement spectrum.

The entanglement entropies features commented above are independent of the exchange symmetry. Nevertheless, when some particular symmetry is chosen there are several aspects that need further discussion. We use bosons and fermions in the sense that the eigenfunctions are symmetrical or antisymmetrical with respect to coordinate interchange, but in two dimensions the permutation group actually corresponds to the more diverse braid group.

The eigenvalues of the reduced density matrix for the one-dimensional case for both bosons and fermions show two well-defined regimes. In one regime a given eigenvalue λ_m becomes null for some values of ν; in the other one it is fairly independent of ν and λ_m seems to obey $\lambda_m \sim a^m$ with $a > 0$. Besides, in the second regime, the natural occupation numbers of bosons and fermions have the same asymptotic values in the large-interaction limit. Both features (the power law and the asymptotic degeneracy) have already been noted by Schilling in his analysis of the one-dimensional harmonium [7].

In two-dimensional models the natural occupation numbers of bosons and fermions show the same scenario described in the previous paragraph. However, the two-dimensional case presents a fundamental difference with respect to the one-dimensional model because the fermion ground state is twofold degenerate. So, any function in this two-dimensional functional space, Eq. (23), is a ground state with a particular value of the von Neumann entropy. Our results indicate a remarkable physical trait: the fermion states whose von Neumann entropy asymptotically approaches the boson's von Neumann entropy are those that are also eigenstates of the angular momentum. Moreover, the von Neumann entropy is maximal for these states, as shown in Fig. 5(b).

The analysis of Fig. 5 has led us to think that they can be a particular example of a very general result concerning the von Neumann entropy of degenerate states. We guess that states with more symmetry, as those as $\psi_S^{\pm}$ with respect to $\psi_S^{x,y}$, will always have larger von Neumann entropies than those with less symmetry irrespective of the number of particles and particular features of the Hamiltonian. More precisely, if $\mathcal{O}$ is an observable which commutes with the Hamiltonian, $[H,\mathcal{O}] = 0$, and $\psi_{k,l}$, with $l = 1,\ldots,L$ are degenerate eigenfunctions of the Hamiltonian,

$$H\psi_{k,l} = E_k\psi_{k,l}, \tag{56}$$

and eigenfunctions of

$$\mathcal{O}\psi_{k,l} = \theta_l\psi_{k,l}, \tag{57}$$

then $S_{vN}[\psi_{k,1}] = \cdots = S_{vN}[\psi_{k,L}]$ and is a maximum over $S_{vN}[\psi]$ with $\psi \in \mathcal{B} = \text{span}\{\psi_{k,l}\}$. Moreover, the minima correspond to the set of equally weighted superpositions

$$\psi_{\min} = \frac{1}{\sqrt{L}}\sum_{l=1}^{L} e^{i\varphi_l}\psi_{k,l}. \tag{58}$$

The propositions stated above are valid for all the systems we analyzed using numerical methods, prompting us to work on a proof along these lines.

ACKNOWLEDGMENT

We acknowledge SECYT-UNC and CONICET for partial financial support.

[1] N. Killoran, M. Cramer, and M. B. Plenio, Phys. Rev. Lett. **112**, 150501 (2014).
[2] F. Iemini and R. O. Vianna, Phys. Rev. A **87**, 022327 (2013).
[3] N. Helbig, I. V. Tokatly, and A. Rubio, Phys. Rev. A **81**, 022504 (2010).
[4] O. Osenda, F. M. Pont, A. Okopińska, and P. Serra, J. Phys. A: Math. Theor. **48**, 485301 (2015).
[5] H. Katsura and Y. Hatsuda, J. Phys. A: Math. Theor. **40**, 13931 (2007).
[6] C. L. Benavides-Riveros, I. V. Toranzo, and J. S. Dehesa, J. Phys. B: At., Mol. Opt. Phys. **47**, 195503 (2014).
[7] C. Schilling, Phys. Rev. A **88**, 042105 (2013).
[8] P. Kościk and A. Okopińska, Few-Body Syst. **54**, 1637 (2013).
[9] M. Moshinsky, Am. J. Phys. **36**, 52 (1968).
[10] F. Calogero, J. Math. Phys. **10**, 2191 (1969).
[11] B. Sutherland, J. Math. Phys. **12**, 246 (1971).
[12] B. D. Simons, P. A. Lee, and B. L. Altshuler, Phys. Rev. Lett. **70**, 4122 (1993).

[13] B. D. Simons and B. L. Altshuler, Phys. Rev. B **48**, 5422 (1993).
[14] H. Azuma and S. Iso, Phys. Lett. B **331**, 107 (1994).
[15] M. V. N. Murthy and R. Shankar, Phys. Rev. Lett. **73**, 3331 (1994).
[16] A. P. Polychronakos, J. Phys. A: Math. Gen. **39**, 12793 (2006).
[17] A. P. Polychronakos, Phys. Rev. Lett. **70**, 2329 (1993).
[18] C. L. Benavides-Riveros, J. M. Gracia-Bondía, and M. Springborg, Phys. Rev. A **88**, 022508 (2013).
[19] R. Chakraborty and D. A. Mazziotti, Phys. Rev. A **89**, 042505 (2014).
[20] C. Schilling, Phys. Rev. A **91**, 022105 (2015).
[21] K. J. H. Giesbertz and R. van Leeuwen, J. Chem. Phys. **139**, 104109 (2013).
[22] D. Manzano, A. R. Plastino, J. S. Dehesa, and T. Koga, J. Phys. A: Math. Theor. **43**, 275301 (2010).
[23] O. Osenda and P. Serra, Phys. Rev. A **75**, 042331 (2007).
[24] B. Zeng, H. Zhai, and Z. Xu, Phys. Rev. A **66**, 042324 (2002).
[25] S. Iblisdir, J. I. Latorre, and R. Orús, Phys. Rev. Lett. **98**, 060402 (2007).
[26] M. Haque, O. Zozulya, and K. Schoutens, Phys. Rev. Lett. **98**, 060401 (2007).
[27] P. Calabrese, M. Mintchev, and E. Vicari, Phys. Rev. Lett. **107**, 020601 (2011).
[28] P. Calabrese, M. Mintchev, and E. Vicari, J. Stat. Mech. (2011) P09028.
[29] V. Alba, L. Tagliacozzo, and P. Calabrese, Phys. Rev. B **81**, 060411 (2010).
[30] P. J. Forrester and S. O. Warnaar, Bull. Am. Math. Soc. **45**, 489 (2008).
[31] A. Khare, Phys. Lett. A **245**, 14 (1998).
[32] O. Osenda, P. Serra, and S. Kais, Int. J. Quantum Inf. **06**, 303 (2008).
[33] M. Altunbulak and A. Klyachko, Commun. Math. Phys. **282**, 287 (2008).
[34] P. Kościk, Phys. Lett. A **379**, 293 (2015).
[35] F. M. Pont, O. Osenda, J. H. Toloza, and P. Serra, Phys. Rev. A **81**, 042518 (2010).
[36] L. Amico, R. Fazio, A. Osterloh, and V. Vedral, Rev. Mod. Phys. **80**, 517 (2008).
[37] O. Osenda and G. A. Raggio, Phys. Rev. A **72**, 064102 (2005).
[38] See Supplemental Material at http://link.aps.org/supplemental/10.1103/PhysRevA.94.042115 for the numerical evidence of the analytic behavior of the one-particle reduced density matrix eigenvalues.
[39] A. Hamma, L. Cincio, S. Santra, P. Zanardi, and L. Amico, Phys. Rev. Lett. **110**, 210602 (2013).
[40] J. Cui, L. Amico, H. Fan, M. Gu, A. Hamma, and V. Vedral, Phys. Rev. B **88**, 125117 (2013).
[41] F. Franchini, J. Cui, L. Amico, H. Fan, M. Gu, V. Korepin, L. C. Kwek, and V. Vedral, Phys. Rev. X **4**, 041028 (2014).
[42] S. Santra, A. Hamma, L. Cincio, Y. Subasi, P. Zanardi, and L. Amico, Phys. Rev. B **90**, 245128 (2014).
[43] P. Kościk and A. Okopińska, Phys. Lett. A **374**, 3841 (2010).
[44] D. F. V. James, Appl. Phys. B: Lasers Opt. **66**, 181 (1998).
[45] K. Balzer *et al.*, J. Phys.: Conf. Ser. **35**, 209 (2006).
[46] F. G. Tricomi, *Integral Equations* (Interscience Publishers, London, 1957).